A Control Scheme for Automatic Path Tracking of Vehicles Subject to Wheel Slip Constraint

Shou-Tao Peng, Jer-Jia Sheu and Chau-Chin Chang
Department of Mechanical Engineering,
Southern Taiwan University of Technology, Tainan, Taiwan.

***Abstract*—In this paper we present a control scheme for automatic path tracking of a four-wheeled steering and four-wheeled drive (4WS4WD) vehicle subject to wheel slip constraint. The wheel slip, containing wheel slip ratio in longitudinal direction and slip angle in lateral direction, is a vector that serves as an index to avoid the tire-road friction saturation. Using linearization and singular perturbation theory, a linear and order-reduced design model is obtained, and the wheel slip is replaced by its quasi-steady state for the controller design. We propose a control structure of wheel torque and steering to transform the original tracking problem to a problem of state regulation subject to input constraint. A low-and-high gain technique is applied to construct the constrained controller and to enhance the utilization of the constrained wheel slip. Simulation shows that the new proposed control scheme subject to wheel slip constraint coordinates well between wheel steering and wheel torque during tracking.**

1 Introduction

Controller design for a vehicle to track a desired path without tire-road friction saturation is an important issue in vehicle intelligent cruise control. Saturation of tire-road friction, which is associated with magnitude of the wheel slip, quite often leads to skidding and causes vehicle instability in a slippery road condition. The wheel slip under study is a vector that provides information about magnitude and direction of friction force [1]. When the magnitude of the wheel slip exceeds the critical value related to road condition, the friction force will saturate. Most of the controller designs consider wheel slip ratio and slip angle separate, only few of the designs combine them with some complicated modifications (see [2]-[6] and references therein). In this paper, the wheel slip is treated in a unified manner and the notion of constraining the wheel slip is applied to avoid friction saturation.

As being aware of the fast and locally input-to-state stability (ISS) of the wheel subsystem, we use linearization and singular perturbation theory [7] to obtain a simplified design model and regard the quasi-steady state of wheel slip as the constraint target to develop the controller. Based on the design model, a control structure of the wheel torque and steering is proposed. This control structure is composed of two parts: one is used for decoupling, and the other part is used for manipulating as well as limiting the wheel slip. By using the control structure, the original tracking problem can be transformed to a problem of state regulation subject to input constraint, which can be solved by applying a framework of semiglobal stabilization (see [8] and references therein). Our constrained controller is designed with a low-and-high gain technique by which utilization of the wheel slip under constraint is enhanced, and so that the tracking performances, such as regulation rate and disturbance rejection, can be improved. Uncertainty of tire-road conditions for robustness issue is also considered.

Simulation shows that the proposed control scheme during tracking is capable of limiting the wheel slip, and has a satisfactory coordination between wheel torque and wheel steering. During the transient, the scheme can automatically provide auxiliary differential wheel torque to improve the cornering performance, and furthermore, can provide wheel torque persistently to avoid vehicle speed reduction due to the cornering resistance.

2 Vehicle system model

2.1 Modeling of vehicle and path for tracking

As shown in Fig. 1, a 4WS4WD vehicle with a reference path for tracking is considered as a vehicle system that comprises three subsystems: namely, vehicle body, four wheels, and kinematics between the vehicle and the path.

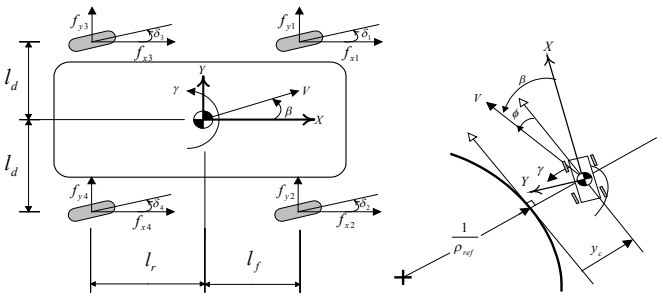

Figure 1. Vehicle system and tracking path

Variables used for the vehicle body are the center of gravity (CG) speed $v = \|V\|$, the sideslip angle β, and the yaw rate γ. Variables for the wheels are the wheel angular speeds ω_j ($j = 1,...,4$). Generalized coordinates describing the kinematics are the perpendicular distance y_c and the angle ϕ between the direction of vehicle velocity and the tangent to the path curve. The dynamical equations for these subsystems can be expressed as follows:

2.1.1 Vehicle body dynamics

$$\begin{bmatrix} m & 0 & 0 \\ 0 & mv & 0 \\ 0 & 0 & J_z \end{bmatrix} \frac{d}{dt} \begin{bmatrix} v \\ \beta \\ \gamma \end{bmatrix} = \begin{bmatrix} \cos\beta & \sin\beta & 0 \\ -\sin\beta & \cos\beta & 0 \\ 0 & 0 & 1 \end{bmatrix} \sum_{j=1}^{4} \begin{bmatrix} f_{xj} \\ f_{yj} \\ M_{zj} \end{bmatrix} - \begin{bmatrix} 0 \\ mv\gamma \\ 0 \end{bmatrix} \quad (1a)$$

$$\sum_{j=1}^{4} M_{zj} = [-l_d \quad l_f][f_{x1} \quad f_{y1}]' + [l_d \quad l_f][f_{x2} \quad f_{y2}]' + [-l_d \quad -l_r][f_{x3} \quad f_{y3}]' + [l_d \quad -l_r][f_{x4} \quad f_{y4}]' \quad (1b)$$

where f_{xj}, f_{yj}, and M_{zj}, $j = 1,..,4$, defined in the body-fixed $X-Y-Z$ coordinate, are external forces and yaw moments that mainly results from the tire-road friction. Notations m and J_z are respectively the mass of vehicle and the inertia about Z axis. Symbols l_f, l_r, and l_d are respectively the distances measured from the CG to the front, the rear axles, and to the wheel side.

2.1.2 Wheel dynamics

$$I_{wj} \frac{d}{dt} \omega_j = T_j - r_{ej} \begin{bmatrix} \cos\delta_j & \sin\delta_j \end{bmatrix} \begin{bmatrix} f_{xj} \\ f_{yj} \end{bmatrix} \quad (2)$$

where I_{wj} and r_{ej} represent the inertia and effective radius of the wheel j respectively, and T_j, δ_j are the wheel torque and steering angle used for control scheme.

2.1.3 Interaction between vehicle and path during tracking

Kinematics of the interaction can be derived as

$$\dot{y}_c = -v\sin\phi \tag{3a}$$

$$\dot{\phi} = -\frac{v}{(1/\rho_{ref}) + y_c}\cos\phi + \dot{\beta} + \gamma \tag{3b}$$

where the path curvature ρ_{ref} is given and assumed to be constant for easily demonstrating the proposed control scheme.

2.2 Calculation of friction force

To calculate the friction forces due to tire-road interaction, we need to know the normal load transfer, wheel slip, and friction coefficient of each wheel. A scheme [1] to calculate the wheel slip and the related friction coefficient is adopted in this article; because it is useful for analytical study on the friction saturation and on the vehicle system linearization.

2.2.1 Normal load transfer

The normal loads on the four wheels are given as [4]

$$\begin{aligned}
f_{z1} &= \frac{l_r}{l_f+l_r}\frac{mg}{2} - \frac{h}{l_f+l_r}\frac{ma_x}{2} - \frac{k_{f\phi}}{k_{f\phi}+k_{r\phi}}\frac{h}{l_d}\frac{ma_y}{2} \\
f_{z2} &= \frac{l_r}{l_f+l_r}\frac{mg}{2} - \frac{h}{l_f+l_r}\frac{ma_x}{2} + \frac{k_{f\phi}}{k_{f\phi}+k_{r\phi}}\frac{h}{l_d}\frac{ma_y}{2} \\
f_{z3} &= \frac{l_f}{l_f+l_r}\frac{mg}{2} + \frac{h}{l_f+l_r}\frac{ma_x}{2} - \frac{k_{r\phi}}{k_{f\phi}+k_{r\phi}}\frac{h}{l_d}\frac{ma_y}{2} \\
f_{z4} &= \frac{l_f}{l_f+l_r}\frac{mg}{2} + \frac{h}{l_f+l_r}\frac{ma_x}{2} + \frac{k_{r\phi}}{k_{f\phi}+k_{r\phi}}\frac{h}{l_d}\frac{ma_y}{2}
\end{aligned} \tag{4a}$$

where h denotes the height of CG; g is the gravitational constant; $k_{f\phi}$ and $k_{r\phi}$ are respectively the front and rear roll stiffness; a_x and a_y denote the longitudinal and lateral acceleration of the vehicle body respectively and can be obtained by Newton's Law as

$$a_x = \sum_{j=1}^{4} f_{xj}/m\,,\ a_y = \sum_{j=1}^{4} f_{yj}/m \tag{4b}$$

2.2.2 Wheel slip

To calculate the wheel slip S_j (see Fig. 2), we need to know, in addition, the wheel center velocity V_j and the slip angle α_j. The V_j of each wheel j is calculated by

$$\begin{aligned}
V_1 &= \begin{bmatrix} v_{x1} \\ v_{y1} \end{bmatrix} = \begin{bmatrix} v\cos\beta - l_d\gamma \\ v\sin\beta + l_f\gamma \end{bmatrix},\ V_2 = \begin{bmatrix} v_{x2} \\ v_{y2} \end{bmatrix} = \begin{bmatrix} v\cos\beta + l_d\gamma \\ v\sin\beta + l_f\gamma \end{bmatrix} \\
V_3 &= \begin{bmatrix} v_{x3} \\ v_{y3} \end{bmatrix} = \begin{bmatrix} v\cos\beta - l_d\gamma \\ v\sin\beta - l_r\gamma \end{bmatrix},\ V_4 = \begin{bmatrix} v_{x4} \\ v_{y4} \end{bmatrix} = \begin{bmatrix} v\cos\beta + l_d\gamma \\ v\sin\beta - l_r\gamma \end{bmatrix}
\end{aligned} \tag{5}$$

Based on the V_j, the α_j can be calculated as

$$\alpha_j = \delta_j - \beta_j,\ \beta_j = \tan^{-1}\left(v_{yj}/v_{xj}\right), \tag{6}$$

where β_j in terminology is the sideslip angle of wheel j.

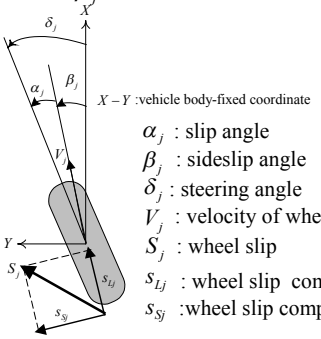

Figure 2. The coordinates and angles for calculating wheel slip

The wheel slip S_j has two components, s_{Lj} and s_{Sj}, that are defined respectively along and perpendicular to the direction of velocity V_j [1]. The wheel slip is characterized by

$$S_j = \begin{bmatrix} s_{Lj} \\ s_{Sj} \end{bmatrix} = \frac{1}{\max\left(r_{ej}\omega_j\cos\alpha_j, \|V_j\|\right)} \begin{bmatrix} r_{ej}\omega_j\cos\alpha_j - \|V_j\| \\ r_{ej}\omega_j\sin\alpha_j \end{bmatrix} \tag{7}$$

2.2.3 Tire model for friction force

The friction force on the tire of wheel j is given as

$$\begin{bmatrix} f_{xj} & f_{yj} \end{bmatrix}' = f_{zj}\begin{bmatrix} \mu_{xj} & \mu_{yj} \end{bmatrix}' \tag{8}$$

where f_{zj} is the normal load defined by Eq. (4a) and $\begin{bmatrix} \mu_{xj} & \mu_{yj} \end{bmatrix}'$ is the friction coefficient calculated as

$$\begin{bmatrix} \mu_{xj} \\ \mu_{yj} \end{bmatrix} = \begin{bmatrix} \cos\beta_j & -\sin\beta_j \\ \sin\beta_j & \cos\beta_j \end{bmatrix} \begin{bmatrix} \mu_{Lj} \\ \mu_{Sj} \end{bmatrix}, \tag{9}$$

$$\begin{bmatrix} \mu_{Lj} \\ \mu_{Sj} \end{bmatrix} = \begin{bmatrix} 1 & 0 \\ 0 & k_{sj} \end{bmatrix} \mu_{\mathrm{Res}}\left(\|S_j\|\right)\frac{S_j}{\|S_j\|}. \tag{10}$$

In Eq. (9), the friction coefficient $\begin{bmatrix} \mu_{xj} & \mu_{yj} \end{bmatrix}'$, described in the vehicle body-fixed coordinate, is transformed from a coordinate $\begin{bmatrix} \mu_{Lj} & \mu_{Sj} \end{bmatrix}'$ with a basis same as the wheel slip S_j. In Eq. (10), $k_{sj} \in [0.9,\ 0.95]$ is a factor that is used for attenuation in presence of tire tread profile. The scalar μ_{Res} is a saturation function of variables $\|S_j\|$ and road conditions. When the magnitude of wheel slip $\|S_j\|$ exceeds the threshold associated with road condition, the μ_{Res} saturates and shrinks, and so does the related friction force in Eq. (8). Conversely, the saturation of friction force can be avoided, provided the magnitude of wheel slip is limited below the related threshold. For analytic purpose, it is commonly assumed that μ_{Res} has the following features around $\|S_j\| = 0$:

(1) $$\mu_{\mathrm{Res}}\left(\|S_j\|\right)_{\|S_j\|=0} = 0 \tag{11}$$

(2) $$\left.\frac{\partial\mu_{\mathrm{Res}}\left(\|S_j\|\right)}{\partial\|S_j\|}\right|_{\|S_j\|=0} = \lim_{\|S_j\|\to 0_+}\frac{\mu_{\mathrm{Res}}\left(\|S_j\|\right)}{\|S_j\|} \triangleq k_j \tag{12}$$

The initial slope k_j in Eq. (12) depends mainly on road conditions. A better road condition gives a larger slope k_j and in turn provides a larger friction coefficient. Notably Eqs. (4a), (4b), and (8) can be linked as a feedback connection, thus the transfer (4a) can be rewritten as

$$F_z = (I_4 + GN)^{-1}F_{zs} \tag{13a}$$

where I_4 is the 4×4 identity matrix and

$$F_z = \begin{bmatrix} f_{z1} & f_{z2} & f_{z3} & f_{z4} \end{bmatrix}',\ N = \begin{bmatrix} \mu_{x1} & \mu_{x2} & \mu_{x3} & \mu_{x4} \\ \mu_{y1} & \mu_{y2} & \mu_{y3} & \mu_{y4} \end{bmatrix},$$

$$G = \frac{h}{2l_d}\begin{bmatrix} \frac{l_d}{l_f+l_r} & \frac{l_d}{l_f+l_r} & \frac{-l_d}{l_f+l_r} & \frac{-l_d}{l_f+l_r} \\ \frac{k_{f\phi}}{k_{f\phi}+k_{r\phi}} & \frac{-k_{f\phi}}{k_{f\phi}+k_{r\phi}} & \frac{k_{r\phi}}{k_{f\phi}+k_{r\phi}} & \frac{-k_{r\phi}}{k_{f\phi}+k_{r\phi}} \end{bmatrix}',$$

$$F_{zs} = [f_{zs1}\ f_{zs2}\ f_{zs3}\ f_{zs4}]' = \frac{mg}{2}\begin{bmatrix} \frac{l_r}{l_f+l_r} & \frac{l_r}{l_f+l_r} & \frac{l_f}{l_f+l_r} & \frac{l_f}{l_f+l_r} \end{bmatrix}' \tag{13b}$$

In Eq. (13), F_z and F_{zs} are referred to as the dynamic and static normal load respectively.

3 Linear design model

3.1 Linearization with model reduction

The previous nonlinear vehicle system and tire model that we consider are linearized around the following free rolling condition:

$\rho_{ref\,0}=0$, $\|V_0\|=v_0$, $\beta_0=0$, $\gamma_0=0$, $w_{j0}=v_0/r_{ej}$, $y_{c0}=0$, $\phi_0=0$,

$\delta_{j0}=0$, $T_{j0}=0$, $j=1,...,4$.

Using typical vehicle data to characterize the linearization indicates that, as compared to the other two subsystems, the resulting linearized wheel subsystem

$$\left(\frac{I_{wj}v_0}{r_{ej}^2k_jf_{zsj}}\right)\frac{d}{dt}\partial\omega_j=-\partial\omega_j+\frac{1}{r_{ej}}\left(\partial v+(-1)^j\gamma l_d\right)+\frac{v_0}{r_{ej}^2k_jf_{zsj}}T_j$$

is much faster and ISS, where $\partial v\triangleq v-v_0$, $\partial\omega_j\triangleq\omega_j-\omega_{j0}$, and k_j, f_{zsj} respectively are the slope (12) and static normal load (13b). Hence based on the singular perturbation theory [7], the linearization can be simplified by replacing the wheel subsystem with its quasi-steady state

$$\partial\omega_j=\frac{1}{r_{ej}}\left(\partial v+(-1)^j\gamma l_d\right)+\frac{v_0}{r_{ej}^2k_jf_{zsj}}T_j.$$

With the replacement, it can be verified that the following linearized vehicle system and tire model are obtained:

3.2 The linearized vehicle system

$$\frac{d}{dt}\begin{bmatrix}\partial v\\ \beta\\ \gamma\\ y_c\\ \phi\end{bmatrix}=\begin{bmatrix}0&0&0&0&0\\0&0&-1&0&0\\0&0&0&0&0\\0&0&0&0&-v_o\\0&0&0&0&0\end{bmatrix}\begin{bmatrix}\partial v\\ \beta\\ \gamma\\ y_c\\ \phi\end{bmatrix}+\begin{bmatrix}1/m&0&0\\0&1/mv_o&0\\0&0&1/J_z\\0&0&0\\0&1/mv_o&0\end{bmatrix}\sum_{j=1}^{4}\begin{bmatrix}f_{xj}\\ f_{yj}\\ M_{zj}\end{bmatrix}+\begin{bmatrix}0\\0\\0\\0\\-v_o\end{bmatrix}\rho_{ref}\qquad(14)$$

where (f_{xj},f_{yj},M_{zj}) are obtained from the following tire model.

3.3 The linearized tire model

The linearized tire model turns out to be a cascade form. Matrix representation for this cascade form is given by

(1) From the control input (T_j,δ_j) to the quasi-steady state wheel slip $\tilde{S}_j$:

$$\tilde{S}_1=\begin{bmatrix}\dfrac{T_1}{r_{e1}f_{zs1}k_1}\\ -\beta-\dfrac{l_f}{v_0}\gamma+\delta_1\end{bmatrix},\ \tilde{S}_2=\begin{bmatrix}\dfrac{T_2}{r_{e2}f_{zs2}k_2}\\ -\beta-\dfrac{l_f}{v_0}\gamma+\delta_2\end{bmatrix},\ \tilde{S}_3=\begin{bmatrix}\dfrac{T_3}{r_{e3}f_{zs3}k_3}\\ -\beta+\dfrac{l_r}{v_0}\gamma+\delta_3\end{bmatrix},\ \tilde{S}_4=\begin{bmatrix}\dfrac{T_4}{r_{e4}f_{zs4}k_4}\\ -\beta+\dfrac{l_r}{v_0}\gamma+\delta_4\end{bmatrix}\qquad(15)$$

(2) From the $\tilde{S}_j$ to the friction force (f_{xj},f_{yj},M_{zj})

$$\begin{bmatrix}f_{x1}\\ f_{y1}\\ M_{z1}\end{bmatrix}=\begin{bmatrix}1&0\\0&1\\-l_d&l_f\end{bmatrix}\begin{bmatrix}f_{zs1}k_1&0\\0&k_{s1}f_{zs1}k_1\end{bmatrix}\tilde{S}_1,\quad\begin{bmatrix}f_{x2}\\ f_{y2}\\ M_{z2}\end{bmatrix}=\begin{bmatrix}1&0\\0&1\\l_d&l_f\end{bmatrix}\begin{bmatrix}f_{zs2}k_2&0\\0&k_{s2}f_{zs2}k_2\end{bmatrix}\tilde{S}_2,$$

$$\begin{bmatrix}f_{x3}\\ f_{y3}\\ M_{z3}\end{bmatrix}=\begin{bmatrix}1&0\\0&1\\-l_d&-l_r\end{bmatrix}\begin{bmatrix}f_{zs3}k_3&0\\0&k_{s3}f_{zs3}k_3\end{bmatrix}\tilde{S}_3,\quad\begin{bmatrix}f_{x4}\\ f_{y4}\\ M_{z4}\end{bmatrix}=\begin{bmatrix}1&0\\0&1\\l_d&-l_r\end{bmatrix}\begin{bmatrix}f_{zs4}k_4&0\\0&k_{s4}f_{zs4}k_4\end{bmatrix}\tilde{S}_4\qquad(16)$$

We note that if substituting the tire model (15)-(16) into the linearized vehicle system (14), the consequent system has a subsystem of (β,γ) identical to the linear two-track model commonly used in the literature. Also note that in Eq. (16) the terms $f_{zj}k_j$ and $k_{sj}f_{zj}k_j$ can be respectively interpreted as the 'longitudinal stiffness' and 'cornering stiffness' in the literature. Some assumptions for the tire-road condition are given as follows:

Assumption 1: *(tire-road condition)*

(1) All the four tires have the same effective radius and attenuation factor so $r_{ej}\triangleq r_e$, $k_{sj}\triangleq k_s$, $j=1,...,4$.

(2) The vehicle runs on one of the following road conditions:

(a) The μ-split road condition so $k_1=k_3\triangleq k_L$, $k_2=k_4\triangleq k_R$.

(b) The μ-uniform road condition so $k_j\triangleq k$, $j=1,...,4$.

Suppose the linearized and order-reduced design system (14)-(16) can be stabilized by the control input (T_j,δ_j) with state feedback and meanwhile, the magnitude of $\tilde{S}_j$ is ensured below a prescribed constraint s_c. Then, the original high order nonlinear vehicle system can also be locally stabilized using the same control scheme; since Jacobian linearization plus singular perturbation theory guarantees that the local stability can be concluded from the stability of the reduced (slow) system [7]. Moreover, the magnitude of wheel slip can be limited approximately below the constraint s_c due to the fast convergence of the wheel slip S_j to its quasi-steady state $\tilde{S}_j$. Hence in the following sections, we will present a (T_j,δ_j) control scheme to achieve this concept.

4 The development of controller

To control a vehicle to track a path of curvature ρ_{ref} with constant tangent speed v_0, the following ideal state

$$\begin{bmatrix}\partial v_{ss}&\beta_{ss}&\gamma_{ss}&y_{c,ss}&\phi_{ss}\end{bmatrix}'=\Pi\rho_{ref},\ \Pi\triangleq\begin{bmatrix}0&0&v_0&0&0\end{bmatrix}'\qquad(17)$$

is chosen as the set point for state regulation.

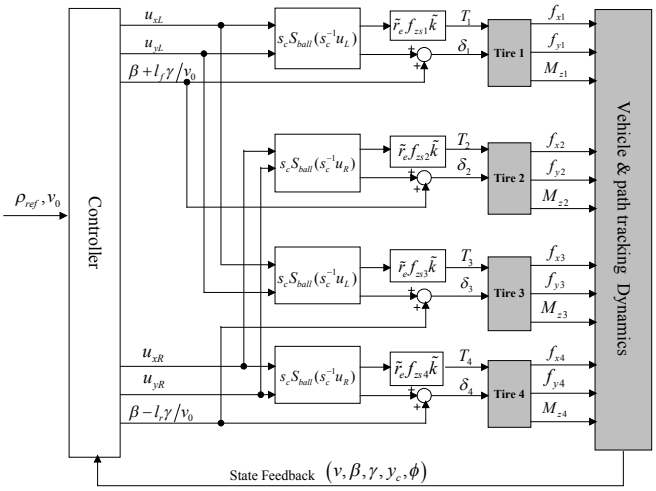

Figure 3. An illustration of the control scheme

4.1 Control structure of the wheel torque and steering

Let $\tilde{r}_e$, $\tilde{k}_s$, $\tilde{k}$ and s_c be respectively the estimated effective radius, attenuation factor of Eq. (10), slope of Eq. (12), and the prescribed constraint for limiting $\|\tilde{S}_j\|$. Define a unit-ball saturation function $S_{ball}:\Re^2\to\Re_+$ as

$$S_{ball}(z)=\begin{cases}z, & \|z\|\le 1\\ z/\|z\|, & \|z\|>1\end{cases},\ z\in\Re^2.\qquad(18)$$

Then as shown in Fig.3, the control structure of the wheel torque and steering is proposed as:

$$\begin{bmatrix} T_1 \\ \delta_1 \end{bmatrix} = \begin{bmatrix} \tilde{r}_e f_{zs1} \tilde{k} & 0 \\ 0 & 1 \end{bmatrix} \left(\begin{bmatrix} 0 \\ \beta + l_f \gamma / v_0 \end{bmatrix} + s_c S_{ball}\left(s_c^{-1} u_L \right) \right), \tag{19a}$$

$$\begin{bmatrix} T_2 \\ \delta_2 \end{bmatrix} = \begin{bmatrix} \tilde{r}_e f_{zs2} \tilde{k} & 0 \\ 0 & 1 \end{bmatrix} \left(\begin{bmatrix} 0 \\ \beta + l_f \gamma / v_0 \end{bmatrix} + s_c S_{ball}\left(s_c^{-1} u_R \right) \right), \tag{19b}$$

$$\begin{bmatrix} T_3 \\ \delta_3 \end{bmatrix} = \begin{bmatrix} \tilde{r}_e f_{zs3} \tilde{k} & 0 \\ 0 & 1 \end{bmatrix} \left(\begin{bmatrix} 0 \\ \beta - l_r \gamma / v_0 \end{bmatrix} + s_c S_{ball}\left(s_c^{-1} u_L \right) \right), \tag{19c}$$

$$\begin{bmatrix} T_4 \\ \delta_4 \end{bmatrix} = \begin{bmatrix} \tilde{r}_e f_{zs4} \tilde{k} & 0 \\ 0 & 1 \end{bmatrix} \left(\begin{bmatrix} 0 \\ \beta - l_r \gamma / v_0 \end{bmatrix} + s_c S_{ball}\left(s_c^{-1} u_R \right) \right), \tag{19d}$$

where (u_L, u_R) is the constrained controller to be defined later. Substituting the control structure (19) into the vehicle system (14)-(16), with Assumption 1, yields

$$\dot{x} = Ax + B(I_4 + \Delta) \begin{bmatrix} S_{ball}(s_c^{-1} u_L) \\ S_{ball}(s_c^{-1} u_R) \end{bmatrix} + \Psi \rho_{ref} \tag{20}$$

where

$$x = \begin{bmatrix} \partial v \\ \beta \\ \gamma \\ y_c \\ \phi \end{bmatrix}, \quad A = \begin{bmatrix} 0 & 0 & 0 & 0 & 0 \\ 0 & 0 & -1 & 0 & 0 \\ 0 & 0 & 0 & 0 & 0 \\ 0 & 0 & 0 & 0 & -v_o \\ 0 & 0 & 0 & 0 & 0 \end{bmatrix}, \quad \Psi = \begin{bmatrix} 0 \\ 0 \\ 0 \\ 0 \\ -v_o \end{bmatrix},$$

$$B = s_c \begin{bmatrix} (f_{zs1} + f_{zs3})\tilde{k}/m & 0 & (f_{zs2} + f_{zs2})\tilde{k}/m & 0 \\ 0 & \tilde{k}_s (f_{zs1} + f_{zs3})\tilde{k}/mv_0 & 0 & \tilde{k}_s (f_{zs2} + f_{zs4})\tilde{k}/mv_0 \\ -l_d (f_{zs1} + f_{zs3})\tilde{k}/J_z & 0 & l_d (f_{zs2} + f_{zs4})\tilde{k}/J_z & 0 \\ 0 & 0 & 0 & 0 \\ 0 & \tilde{k}_s (f_{zs1} + f_{zs3})\tilde{k}/mv_0 & 0 & \tilde{k}_s (f_{zs2} + f_{zs4})\tilde{k}/mv_0 \end{bmatrix},$$

$$\Delta = diag\left(\frac{\tilde{r}_e - r_e}{r_e}, \frac{k_s k_L - \tilde{k}_s \tilde{k}}{\tilde{k}_s \tilde{k}}, \frac{\tilde{r}_e - r_e}{r_e}, \frac{k_s k_R - \tilde{k}_s \tilde{k}}{\tilde{k}_s \tilde{k}} \right), \text{ if } \mu\text{-split}$$

$$\Delta = diag\left(\frac{\tilde{r}_e - r_e}{r_e}, \frac{k_s k - \tilde{k}_s \tilde{k}}{\tilde{k}_s \tilde{k}}, \frac{\tilde{r}_e - r_e}{r_e}, \frac{k_s k - \tilde{k}_s \tilde{k}}{\tilde{k}_s \tilde{k}} \right), \text{ if } \mu\text{-uniform}$$

Note that the rearranged system (20) takes a norm-bounded control (u_L, u_R) and has an uncertain diagonal matrix Δ, which reflects the parametric mismatch between the real and the estimated of the tire-road condition. Properties of the control structure (19) and the rearranged system (20) are summarized as follows:

(a) Property of the control structure (19): *In linear range, manipulating $s_c S_{ball}(s_c^{-1} u_j)$ inside the control structure can be regarded as manipulating $\tilde{S}_j$ of the tire approximately.* This equivalence can be obtained by substituting Eq. (19) into Eq. (15) with the estimated values being selected as $\tilde{r}_e \tilde{k} \approx r_e k_j$.

(b) Properties of the system (20):

(P1) *The pair (A, B) is controllable and the eigenvalues of A are all zero and, therefore, locate in the closed left half plane.*

(P2) *For the set point (17), the following matrix equation*

$$A\Pi + B\Gamma + \Psi = 0_{5\times 1} \tag{21}$$

has a solution

$$\Gamma = \frac{mv_0^2}{\tilde{k}_s \tilde{k} s_c \sum_{j=1}^{4} f_{zsj}} \begin{bmatrix} 0 & 1 & 0 & 1 \end{bmatrix}' \tag{22}$$

(P3) *The diagonal uncertainty matrix Δ can be set positive definite by choosing the estimated parameters as*

$\tilde{r}_e > r_e$, $\tilde{k}_s < k_s$, $\tilde{k} < Min(k_L, k_R, k)$.

In Eq. (22), the denominator term $\tilde{k}_s \tilde{k} s_c \sum_{j=1}^{4} f_{zsj}$ can be viewed as "*the allowed maximum sum of the nominal lateral friction force, limited by the prescribed wheel slip constraint s_c*". In this study, the limited sum $\tilde{k}_s \tilde{k} s_c \sum_{j=1}^{4} f_{zsj}$ is required to be greater than the centrifugal force $mv_0^2 \rho_{ref}$ used in the desired cornering motion. More specifically, the ratio $\tilde{\delta}$ below must satisfy

$$1 > \tilde{\delta} \triangleq \frac{\left| mv_0^2 \rho_{ref} \right|}{\tilde{k}_s \tilde{k} s_c \sum_{j=1}^{4} f_{zsj}} \tag{23}$$

The requirement to make Eq. (23) admissible is equivalent to the following assumption:

Assumption 2: The matrix Γ of Eq. (22) is assumed to satisfy

$$1 > \tilde{\delta} \triangleq Max\left\{ \left\| E_1 \Gamma \rho_{ref} \right\|, \left\| E_2 \Gamma \rho_{ref} \right\| \right\} \tag{24}$$

where

$$E_1 \triangleq \begin{bmatrix} I_2 & 0_{2\times 2} \end{bmatrix}, \; E_2 \triangleq \begin{bmatrix} 0_{2\times 2} & I_2 \end{bmatrix} \tag{25}$$

4.2 The constrained controller design

In this section, we develop the constrained controller (u_L, u_R) to deal with the state regulation problem of the uncertain system (20). For the set point (17), define the regulation error as

$$e = x - \Pi \rho_{ref} \tag{26}$$

By using the system (20) and Eq. (21), the dynamical error equation is obtained as

$$\dot{e} = Ae + B(I_4 + \Delta) \begin{bmatrix} S_{ball}(s_c^{-1} u_L) \\ S_{ball}(s_c^{-1} u_R) \end{bmatrix} - B\Gamma \rho_{ref} \tag{27}$$

To stabilize the error dynamics (27) with norm-bounded control, the constrained controller (u_L, u_R) is proposed as

$$\left. \begin{aligned} u_L &= -s_c (1 + \gamma_H) E_1 B' P_\varepsilon e \\ u_R &= -s_c (1 + \gamma_H) E_2 B' P_\varepsilon e \end{aligned} \right\} \tag{28}$$

where $P_\varepsilon = P_\varepsilon' > 0_{5\times 5}$ and $\gamma_H > 0$ are the design parameters; E_1 and E_2 are the row partition matrices defined in Eq. (25). The design parameter P_ε is the solution of the following algebraic Riccati equation (ARE):

$$A' P_\varepsilon + P_\varepsilon A - P_\varepsilon B B' P_\varepsilon + \varepsilon I_5 = 0_{5\times 5} \tag{29}$$

where $\varepsilon > 0$ is required sufficiently small [8]. For a given solution $(\varepsilon, P_\varepsilon)$ of ARE (29), the design parameter γ_H is chosen sufficiently large so that the linear matrix inequality (LMI)

$$\frac{\tilde{\delta}^2}{\sqrt{\gamma_H}} P_\varepsilon < \varepsilon I_5 + P_\varepsilon B B' P_\varepsilon, \; \frac{1}{\sqrt{\gamma_H}} < \frac{(1 - \tilde{\delta})^2}{\lambda_{\max}(B' P_\varepsilon B)}, \tag{30}$$

is satisfied. The LMI (30) is always feasible since its right hand side is fixed and strictly positive definite, and its left hand side can be set arbitrarily small by enlarging the γ_H. Choosing $(\varepsilon, P_\varepsilon, \gamma_H)$ in the manner above is known as a low-and-high gain technique developed for input constraint in the literature (see [8] and references therein). By this technique, the utilization of the constrained control, i.e., the constrained wheel slip in this study, can be enhanced and in addition, performance issues such as convergence rate and disturbance rejection can be improved. By

substituting the control (28) into system (27), the 'actual control' becomes

$$\begin{bmatrix} S_{ball}\left(-(1+\gamma_H)E_1B'P_\varepsilon e\right) \\ S_{ball}\left(-(1+\gamma_H)E_2B'P_\varepsilon e\right) \end{bmatrix} \tag{31}$$

In particular, when the regulation error e is sufficiently large, the 'actual control' (31) turns out to be

$$S_{ball}\left(-(1+\gamma_H)E_1B'P_\varepsilon e\right)=\frac{-E_1B'P_\varepsilon e}{\left\|E_1B'P_\varepsilon e\right\|},\quad S_{ball}\left(-(1+\gamma_H)E_2B'P_\varepsilon e\right)=\frac{-E_2B'P_\varepsilon e}{\left\|E_2B'P_\varepsilon e\right\|}$$

In this condition, the control (31) behaves as a generalized sliding mode control scheme that tends to robustly stabilize uncertain systems using all its available input capacity.

4.3 Stability analysis

Let $V=e'P_\varepsilon e$ be the Lyapunov function candidate. Then, the Lyapunov derivative $\dot{V}$ of the uncertain system (27) under the control (28) can be written as

$$\dot{V}=e'(A'P_\varepsilon+P_\varepsilon A)e+2e'P_\varepsilon B\begin{bmatrix} S_{ball}\left(-(1+\gamma_H)E_1B'P_\varepsilon e\right) \\ S_{ball}\left(-(1+\gamma_H)E_2B'P_\varepsilon e\right) \end{bmatrix}$$
$$-2e'P_\varepsilon B\Gamma\rho_{ref}+2e'P_\varepsilon B\Delta\begin{bmatrix} S_{ball}\left(-(1+\gamma_H)E_1B'P_\varepsilon e\right) \\ S_{ball}\left(-(1+\gamma_H)E_2B'P_\varepsilon e\right) \end{bmatrix} \tag{32}$$

Using property (P3) and Assumption 2 gives the following Fact 1 and Theorem 1:

Fact 1: The last term of the Lyapunov derivative (32) satisfies

$$2e'P_\varepsilon B\Delta\begin{bmatrix} S_{ball}\left(-(1+\gamma_H)E_1B'P_\varepsilon e\right) \\ S_{ball}\left(-(1+\gamma_H)E_2B'P_\varepsilon e\right) \end{bmatrix}\le 0\,,\ \forall e\in\Re^5$$

Proof. Omitted for brevity.

From the Lyapunov derivative (32), Fact 1 indicates that if the estimated value $(\tilde{r}_e,\tilde{k}_s,\tilde{k})$ is chosen such that the property (P3) is true, then this choice could 'help' the control (28) render the uncertain system (27) more stable in sense of Lyapunov stability.

Theorem 1: The Lyapunov derivative (32) can be estimated as

$\dot{V}<0$, $\forall e\in\{c_1<e'P_\varepsilon e<c_2\}$,

where

$c_1\triangleq 1/\sqrt{\gamma_H}$, $c_2\triangleq(1-\tilde{\delta})^2/\lambda_{\max}(B'P_\varepsilon B)$.

Moreover,

$\lim_{\gamma_H\to\infty}c_1\to 0_+$, $\lim_{\varepsilon\to 0_+}c_2\to\infty$.

Proof. Omitted for brevity.

Theorem 1 gives an estimate of the stability region established by the constrained control (28) and indicates that the state feedback system (27)-(28) has a region of positive invariance $L_V(c_2)=\{e'P_\varepsilon e<c_2\}$ and a region of ultimate boundedness $L_V(c_1)=\{e'P_\varepsilon e\le c_1\}$ so that

$$\forall e(0)\in L_V(c_2)\Rightarrow e(t)\in L_V(c_2),\forall t\ge 0\Rightarrow\lim_{t\to\infty}e(t)\in L_V(c_1)\,.$$

Moreover, theorem 1 indicates that the regions of ultimate boundedness and of positive invariance respectively can be set arbitrarily small and large, as long as the design parameters ε is sufficiently small and γ_H is sufficiently large. However, we note that the proposed design as well as the associated stability analysis is established via linearization approach; hence, only local stabilization can be theoretically guaranteed for the original nonlinear system. While, since the proposed control scheme can act as a sliding mode controller to some extent, its potential in locally coping with the nonlinearity not yet discussed can be expected. Finally, by substituting the constrained controller (28) into the control structure (19), the control design is accomplished.

5 Simulation results

The nonlinear vehicle model presented in section 2 is used for the simulation, in which the friction lag [4] is also included. The vehicle data is given as: $m=1480\,\text{kg}$, $J_z=1950\,\text{kg}\cdot\text{m}^2$, $l_f=1.421\,\text{m}$, $l_r=1.029\,\text{m}$, $l_d=0.751\,\text{m}$, $g=9.81\,\text{m/s}^2$, $h=0.42\,\text{m}$, $k_{f\phi}=50539\,\text{N/rad}$, $k_{r\phi}=20972\,\text{N/rad}$, $r_{ej}=0.31\,\text{m}$, $I_{wj}=0.7\,\text{kg}\cdot\text{m}^2$, $k_s=0.9$, $v_0=28\,\text{m/sec}$. The tracking path is assumed to be a circle of curvature $\rho_{ref}=1/400$ and covered with wet asphalt on left side and dry asphalt on right side (i.e. μ-split condition). The vehicle starts the path tracking with $v(0)=28\,\text{m/sec}$, $\beta(0)=0\text{rad}$, $\gamma(0)=0\text{rad/sec}$, $y_c(0)=30\text{m}$, $\phi(0)=0$ rad and $\omega_j(0)=90.3226\text{rad/sec}$. In accordance with the data of the vehicle and that of the road surface [1], the estimated values $\tilde{r}_e=0.34$, $\tilde{k}_s=0.8$, $\tilde{k}=14.3$, and constraint $s_c=0.05$ are chosen such that property (P3) and Assumption 2 are satisfied, and $\tilde{\delta}=0.3488<1$ is calculated. For constructing the controller (28), parameters $\varepsilon=0.001$, $\gamma_H=60$, and the related P_ε are chosen to solve both the ARE (29) and LMI (30). Fig. 4 depicts that the vehicle under the proposed control scheme approaches the desired path gradually. The vehicle path almost overlaps the desired path eventually. Fig. 5 illustrates the corresponding magnitude of wheel slip of four wheels, as well as the speed, the sideslip angle, and the yaw rate of the CG. The magnitudes of each wheel slip in the transient are also shown in Fig. 6, they are almost limited below $s_c=0.05$ during the tracking. The time profiles of the wheel steering angles and wheel torques in coordination are shown in Fig 7 where differential wheel torque scheme to improve yaw rate performance as well as persistent wheel torque to maintain the CG speed can be observed. The transient behaviors of wheel angular speeds and dynamic normal loads are depicted in Fig. 8 for easy reference.

6 Conclusions

A control scheme for automatic path tracking control subject to wheel slip constrained is presented. The control scheme integrates the wheel slip ratio and slip angle together to avoid complicated modification. Using linearization and singular perturbation theory, the linear order-reduced design model is obtained from the nonlinear system and the wheel slip is replaced with its quasi-steady state for controller design. By the proposed unit-ball saturation function to adjust the torque and steering angle of each wheel, the vehicle will track the path automatically. The simulation example demonstrates the effectiveness of the control scheme to limit the wheel slip and to coordinate the wheel steering and wheel torque. During cornering, the wheel steering is automatically integrated with auxiliary differential wheel torque to improve the yaw rate performance. Since the trend of future automobile design is to use independent motors to drive electric cars, hence our proposed scheme could be considered as one of the controllers used for the future electric cars.

7 Acknowledgements

The authors are grateful to the comments from the reviewers and National Science Council of R.O.C. for supporting the research under Grant NSC92-2213-E218-008.

References

[1] Kiencke, U. and Nielsen, L., 2000, Automotive Control Systems, Springer, Berlin.

[2] Peng, H. and Tomizuka, M., 1993, "Preview Control for Vehicle Lateral Guidance in Highway Automation," ASME Trans. J. Dynamic Systems, Measurement, and Control, 115, pp. 678-386.

[3] Guldner, J., Sienel, W., Tan, H. S., and Ackermann, J., 1999, "Robust Automatic Steering Control for Look-Down Reference Systems with Front and Rear Sensors," IEEE transaction on control systems technology, 7(1), pp. 2-11.

[4] Alleyne, A., 1997, "A Comparison of Alternative Intervention Strategies for Unintended Roadway Departure Control," Vehicle System Dynamics, 27, pp. 157-186.

[5] Rajamani, R., Tan, H. S., Law, B. K., and Zhang, W. B., 2000, "Demonstration of Integrated Longitudinal and Lateral Control for the Operation of Automated Vehicles in Platoons", IEEE transaction on control systems technology, 8(4), pp. 695-708.

[6] Lim, E. H. M. and Hedrick, J. K., 1999, "Lateral and Longitudinal Vehicle Control Coupling for Automated Vehicle Operation," Proceedings of the American Control Conference, pp. 3676-3680.

[7] Khalil, H. K., 2003, Nonlinear Systems 3rd Edition, Prentice Hall, Upper Saddle River, NJ.

[8] Saberi, A., Lin, Z. and Teel, A. R., 1996, "Control of Linear Systems With Saturating Actuators," IEEE Transaction of Automatic. Control, 41(3), pp. 368-378.

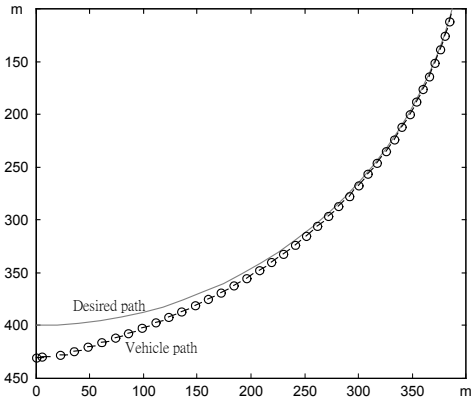

Figure 4

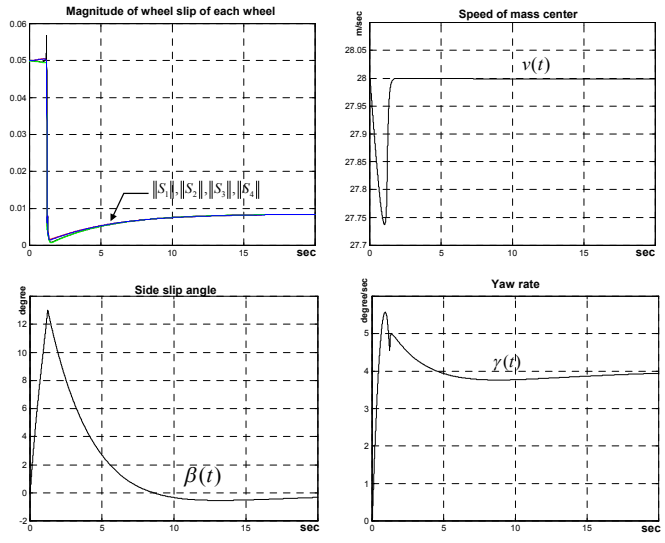

Figure 5

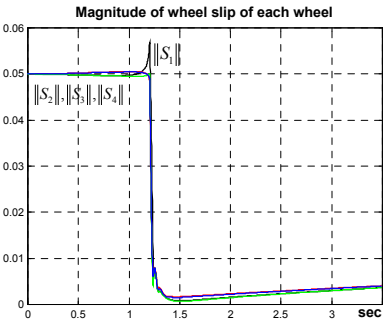

Figure 6

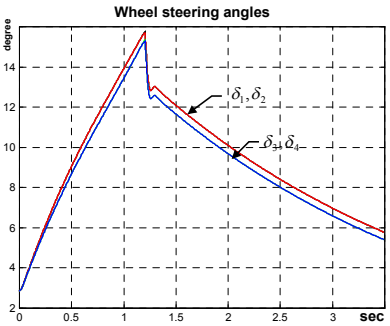

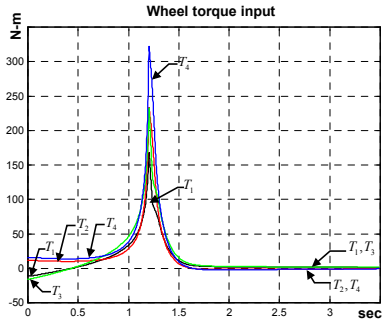

Figure 7

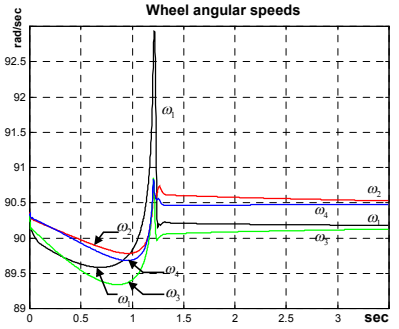

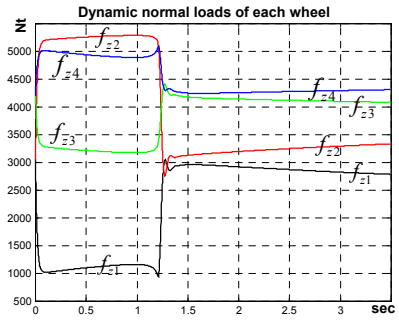

Figure 8